# Toward a Reduced Helium Content Cryogenic Cooling Scheme at 4.5 K for CERN's FCC-hh Accelerator

Patricia Borges de Sousa, Ximo Gallud, Anita Petrovic, Laurent Delprat, Benjamin Bradu, Rob van Weelderen, Laurent Tavian, and Dimitri Delikaris

*(Invited Paper)*

***Abstract*—A conceptual design for cooling superconducting accelerator magnets operating at 4.5 K is proposed for the hadron-hadron configuration of the Future Circular Collider (FCC-hh). This is motivated by efforts to reduce helium inventory and energy costs, while ensuring compatibility with the tunnel structure envisaged for FCC-ee, and providing a technically viable solution for the magnets. The study is carried out for the latest configuration of the FCC-hh machine, the so-called F14 scenario, that uses $Nb_3Sn$ superconducting magnets with an operational magnetic field of 14 T, for a centre-of-mass energy of 85 TeV with a magnetic filling scheme of 83%. The updated heat loads are presented, along with expected longitudinal and radial temperature gradients in the magnet structure. The move from 1.9 K operation, which makes extensive use of He II, towards 4.5 K using single-phase helium significantly reduces the overall cryogenic power consumption by 30%, and the machine's helium inventory by 50%.**

***Index Terms*—Accelerator magnets, magnet cooling, liquid helium, large-scale applications.**

## I. Introduction

THE baseline parameters of the hadron-hadron (-hh) configuration of the Future Cirular Collider at CERN have been updated in the Feasibility Study Report (FSR) [1], published in the first half of 2025, to reflect the so-called F14 scenario [2]. In the latest configuration, the 85 TeV centre-of-mass energy is achieved in a 90.7 km ring populated by 14 T $Nb_3Sn$ dipole magnets at an 83% filling factor [3], [4]; Table I summarises the main parameter changes with respect to the Conceptual Design Report (CDR) [5] and Fig. 1 shows the cryogenic layout for the FCC-hh baseline configuration at 1.9 K.

In the interest of sustainability, an alternative scenario where the $Nb_3Sn$ magnets operate at 4.5 K instead of 1.9 K is evaluated. The main drivers are to reduce overall energy consumption and capital costs, reduce the helium inventory, and to ensure compatibility with the tunnel infrastructure and surface reservation, while providing a viable cooling solution for the magnets. It should however be noted that, as of July 2025, the cooling layout at 1.9 K described in the CDR remains the baseline.

The following sections describe the updated heat loads to the cryogenic system, the reasoning for looking beyond the

TABLE I
Main FCC-hh Parameters for Its Baseline Configuration: Comparison Between the Conceptual Design Report [5] and the Feasibility Study Report [1]

| FCC-hh Parameters | CDR [2019] | FSR [2025] |
|---|---|---|
| Circumference [km] | 97.8 | 90.7 |
| Arc length [km] | 83.8 | 76.9 |
| Operational dipole field [T] | 16 | 14 |
| Centre of mass energy [TeV] | 100 | 85 |
| Synchrotron radiation (2 beams) [MW] | 4.8 | 2.4 |
| Magnet temperature [K] | 1.9 | 1.9 |
| Beam screen temperatures [K] | [40-60] | [40-60] |
| Number of sectors | 10 | 8 |
| Sector length [km] | 9.8 | 11.3 |
| Cryogenic cooling length [km] | 8.4 | 4.9 per side |
| Helium inventory [tonnes] | 880 | 820 |

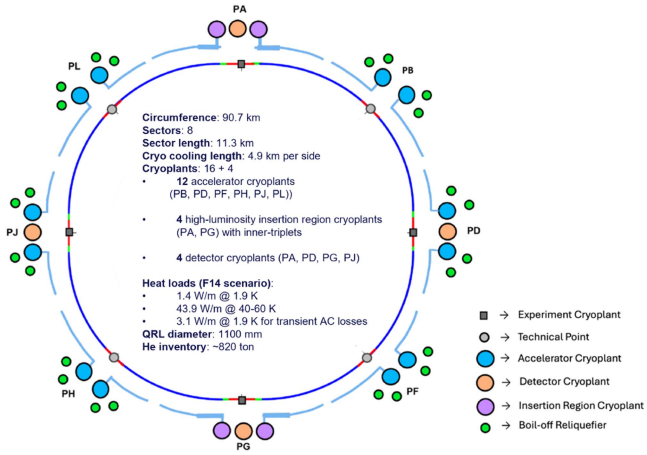


Fig. 1. Updated cryogenic layout of FCC-hh for its baseline configuration at 1.9 K, adapted from [1].

Received 25 July 2025; accepted 22 August 2025. Date of publication 9 September 2025; date of current version 23 September 2025. This work was supported by the High Field Magnets Programme at CERN. *(Corresponding author: Patricia Borges de Sousa.)*

The authors are with CERN, 1211 Geneva, Switzerland (e-mail: pat.borges.sousa@cern.ch).

Color versions of one or more figures in this article are available at https://doi.org/10.1109/TASC.2025.3604763.

Digital Object Identifier 10.1109/TASC.2025.3604763

established cooling strategy at 1.9 K, and introduce the proposed cooling scheme at 4.5 K, highlighting potential advantages and drawbacks. A qualitative evaluation of expected longitudinal and radial temperature gradients in the cold mass is presented and discussed, and future steps to mature the cryogenic layout and fix parameters towards an effective design are outlined.

## II. FCC-hh at 4.5 K

### A. Recap of Baseline Cooling Scheme

The baseline magnet cooling concept for FCC-hh relies on a cryogenic scheme operating at 1.9 K [1], [5], similar to that of the Large Hadron Collider [6]. The cold mass of the accelerator magnets is fully immersed in a static, pressurised bath of He II that transports the heat generated by or deposited onto the magnets to a bayonet heat exchanger carrying saturated He II. In this concept, the additional heat load generated by AC losses due to ramping the magnets up and/or down is buffered by the >30 L/m of pressurised He in the cold mass, which temperature is allowed to increase up to $T_\lambda$. The updated numbers regarding required installed capacity, power consumption and system sizing can be found in [1]. Notably, the overall energy consumption is estimated at 206 MW (for 1040 kW of installed cryogenic capacity at 4.5 $K_{eq}$) and the helium inventory at 820 tonnes.

### B. Why Look Beyond the Baseline?

The motivation to study an alternative to the baseline cooling layout for FCC-hh is to improve its sustainability (and consequently feasibility), by reducing:

- Capital costs;
- operational costs;
- helium inventory.

The authors' proposal involves changing both the magnets' operating temperature and the cryogenic cooling scheme to achieve these goals. Raising the nominal temperature of the arc magnets from 1.9 K to 4.5 K intrinsically improves the thermodynamic efficiency of the cryogenic system, measured in real machines by the inverse coefficient of performance ($COP^{-1}$), *i.e.*, the amount of electrical power input required to produce 1 W of cooling power at a certain temperature. For instance, the effective $COP^{-1}$ of an LHC-like cryoplant is around 960 $W_{elect}/W_{cool}$ at 1.8 K, whereas it decreases to 240 $W_{elect}/W_{cool}$ at 4.5 K [7], [8], resulting in a factor four reduction in electrical consumption for a 2 K change in cooling temperature. While the change from 1.9 K to 4.5 K only slightly reduces the heat loads to the system, it significantly reduces the complexity and capital cost of a cryoplant since there is no production of He II (and hence no need for an array of cold compressors). If the change in operational temperature is coupled to a change in cooling scheme, *e.g.*, from immersion in a bath to forced flow in channels, the overall helium inventory can be reduced by roughly a factor two. More than the cost of helium itself, the reduction in inventory can positively impact the machine's infrastructure and logistics. Namely, it can reduce space reservation at the surface for gas storage during downtime and the frequency of helium deliveries. By having a lower helium content in the cold mass and confining it to cooling channels, the design of the cold mass outer vessel can be revisited, as it no longer serves as a helium containment and pressure vessel, reducing production costs and simplifying quality assurance procedures. As there is less helium in direct contact with the magnet coil, the pressure increase during a quench is limited, and the amount of helium released during a quench event is reduced. The reduction in released helium to the tunnel in such an event is an opportunity to re-define exclusion zones during operation while increasing personnel safety.

In addition to cryogenic aspects, there is evidence that $Nb_3Sn$ magnets designed to operate at 80% of the loadline fraction at 1.9 K can reach the same operational field at 4.5 K, albeit with a lower margin; this has been demonstrated experimentally in bath-cooled magnets only. Moreover, it was observed in these cases that the instabilities limiting performance at 1.9 K are less severe at 4.5 K [3], which may be a further incentive to change the operational temperature to 4.5 K.

TABLE II
Distributed Heat Loads During Nominal Operating Conditions, Including Magnet Powering, Updated to Reflect the FSR

| Heat load @ Temperature level | | 40-60 K [W/m] | 4.5 K [W/m] | 4 K LP [W/m] |
|---|---|---|---|---|
| Static | Supports | 2.4 | 0.13 | |
| | Radiative insulation | | 0.13 | |
| | Thermal shield | 3.1 | | |
| | Feedthrough/vacuum barrier | 0.2 | 0.1 | |
| | Beam screen | | 0.12 | |
| | Distribution | 3.6 | 0.1 | 0.24 |
| | **Total Static** | **9.3** | **0.58** | **0.24** |
| Dynamic | Synchrotron radiation | 31.2 | 0.04 | |
| | Image currents | 3.4 | | |
| | Resistive heating | | 0.3 | |
| | Beam-gas scattering | | 0.45 | |
| | **Total Dynamic** | **34.6** | **0.79** | |
| Transient | AC losses | | 3.13 | |
| **Total without AC losses** | | **43.9** | **1.37** | **0.24** |
| **Total with AC losses** | | **43.9** | **4.5** | **0.24** |

### C. Updated Heat Loads

The distributed heat loads for a standard arc magnet under nominal operating conditions have been reassessed with respect to the updated FSR parameters and collected in Table II.

We assume the same static heat inleaks as the CDR [5], even though they will be slightly lower at 4.5 K than at 1.9 K; numbers will be refined as the magnet design as well as cold mass and beam screen temperature ranges are consolidated. The reduction in centre-of-mass energy and collider circumference have a direct impact on the cryogenic system. The change from 100 TeV to 85 TeV leads to an almost two-fold reduction in the synchrotron radiation intercepted by the beam screen (from 57 W/m to 31.2 W/m) and deposited in the cold mass (from 0.08 W/m to 0.04 W/m). The static + dynamic = steady-state heat loads that need to be extracted from the cold mass during

nominal operation with beam add up to 1.37 W/m. Table II includes the transient (AC) losses generated by ramping the magnets up and down, which are assumed to be 10 kJ/m for a full ramp down-up cycle in 3200 s for a double-aperture dipole, resulting in 3.1 W/m. The value of 10 kJ/m is an aspirational target established by the FCC and HFM studies [5]; current magnet designs using state-of-the-art conductor generate roughly twice the target losses [9]. These transient losses amount to twice the heat loads to be extracted at 4.5 K during steady-state operation and represent a major challenge for the effective sizing of the cryogenic system.

### D. *Cooling at 4.5 K* vs. *1.9 K*

The change in magnet operating temperature must come with a change in cooling strategy. In the LHC, the cold mass is immersed in a pressurized He II bath at 1.9 K that acts as a very effective conduction medium, transporting the heat from the magnet coils to the saturated He II heat exchanger. This cooling scheme provides a remarkable temperature homogeneity, with negligible radial and longitudinal gradients in the cold mass, due to the very large effective thermal conductivity of the pressurized He II bath (roughly 1000 times higher than that of copper at the same temperature [10]). The same cooling concept cannot be applied to an operational temperature of 4.5 K: here, the bulk thermal conductivity of He I is 5-6 orders of magnitude lower than that of He II at 1.9 K, meaning that He I performs worse than metals such as stainless steel at this temperature. Local heat extraction becomes the bottleneck to effective magnet cooling; the need for a change of paradigm in the cooling strategy for accelerator magnets is evident.

Three options arise when discussing cooling at 4.5 K:

- Pool boiling in a saturated bath;
- two-phase (saturated) forced flow;
- single-phase forced flow.

While a saturated bath can provide a nearly isothermal environment for the magnet at low enough heat fluxes, it necessitates a large helium inventory. Other disadvantages include the risk of trapped vapour bubbles in the magnet structure and limited heat transfer by free convection. A cryogenic scheme based on two-phase forced flow of helium in cooling channels inherently comes with a non-negligible radial temperature gradient in the cold mass (typically limited to $<1$ K), but may provide comparable (if not better) heat transfer than pool boiling, depending on flow conditions [11], and with the same longitudinal temperature homogeneity. However, heat transfer in two-phase forced flow is highly dependent on flow patterns within the cooling channel, which can vary along the length and with local heat input, leading to instabilities [12], [13]. Moreover, the slope of the envisaged FCC tunnel can render control of liquid-vapour interfaces challenging [14]. A cooling scheme based on single-phase forced flow in channels can provide excellent heat transfer without the instabilities and slope dependence of a two-phase scheme, at the cost of a longitudinal temperature increase; this can be mitigated by adequate tuning of cryogenic system parameters such as circulating mass flow rate. By confining helium to cooling channels, the inventory in contact with the magnet is drastically reduced, and the overall inventory may be reduced by half with respect to the CDR configuration at 1.9 K, from 820 to 390 tonnes.

Efforts are therefore concentrated on developing an alternative to the baseline cooling scheme, at around 4.5 K by means of forced flow in cooling channels inside the cold mass, using single-phase helium at 0.3 MPa. Although the system pressure can be increased, studies show that heat transfer and available enthalpy difference are optimal at 0.3 MPa when discussing single-phase or supercritical flow [15]. The cryogenic system shall be able to extract steady-state (static+dynamic) as well as transient (ramping) heat loads while keeping the warmest spot on the magnet coils below 5 K, which this is the current design parameter established within the High Field Magnet programme.

### E. *Proposed Cooling Scheme*

A cooling scheme using forced flow of single-phase helium can be implemented either by confining the helium flow to cooling channels embedded into the cold mass, or by allowing the helium stream to flow freely through the entire cold mass cross-section. A similar type of cooling scheme, albeit for lower heat loads, was proposed in 1986 for the Superconducting Super Collider (SSC) [16]; in fact, with the notable exception of the LHC, accelerators like RHIC, HERA, and the Tevatron have all relied on cooling schemes at around 4.5 K for their superconducting magnets [17], [18], [19]. A conceptual layout of the proposed cooling scheme is depicted in Fig. 2.

The single-phase stream of helium at 0.3 MPa and 4.1 K (line 'A' in Fig. 2) circulates through the magnets along the entire cooling sector (4.9 km), warming up as it absorbs the heat generated by or deposited on the magnets; as a result, the magnet at the end of an arc cell sees a higher helium temperature than the one at its start. This intrinsic longitudinal temperature increase is mitigated over the sector at intervals coherent with the cell lattice: the single-phase stream is re-cooled via heat exchange with two-phase helium reservoirs, called "re-coolers" in Fig. 2 at the end of every arc cell. This creates a sawtooth temperature profile in line 'A' (and in the magnets) along the sector and creates a quasi-identical cryogenic environment for each of the cells along the sector (see schematic in Fig. 3). Line 'C' distributes subcooled helium throughout the sector, that gets expanded into the two-phase region to feed each re-cooler. Line 'B' is the recovery line of the re-coolers: its return pressure to the cryoplant imposes the saturation temperature in the re-coolers, and consequently the minimum temperature to which the helium stream in line 'A' can be re-cooled. Currently, a $\Delta T = 0.1$ K is considered between the He stream and the saturated He in the re-coolers. Lines 'E' and 'F' are the supply and return lines for the beam screen and thermal shield cooling circuits, operating at around 5 MPa and from 40 K to 60 K. The beam screen cooling strategy remains identical to what was outlined in the CDR, with the screen and the cold mass thermal shield cooled in series at half-cell increments. Lines 'B', 'C', 'E', and 'F', on the top portion of Fig. 2, make up the cryogenic distribution line (QRL); Line 'F' cools the distribution line's thermal screen on

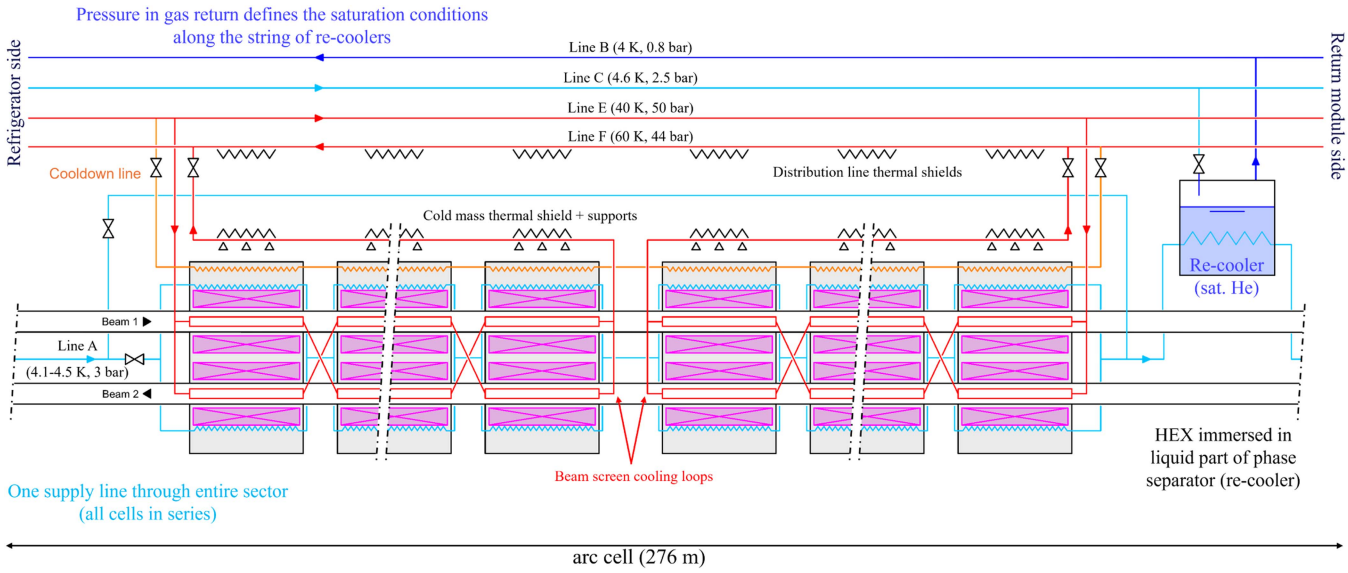


Fig. 2. Cryogenic layout of an arc cell for the proposed cooling scheme at 4.5 K. The cryogenic distribution line includes lines B to F, whereas line A is embedded in the cold masses and runs in series throughout an entire sector. For a 4.9 km cooling sector, there are 18 cell-re-cooler pairs.

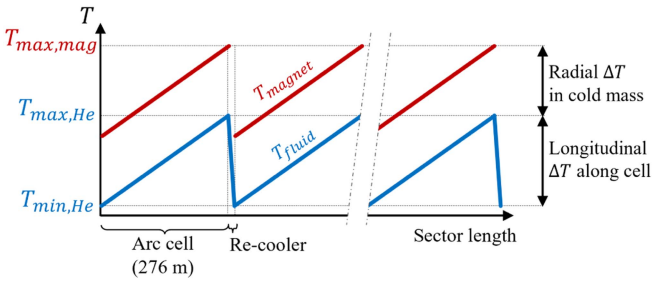


Fig. 3. Typical helium and magnet temperature profile along a cryogenic cooling sector. As heat is extracted from the magnets, the helium temperature increases, until it is re-cooled at the end of every cell back to its original inlet temperature, creating a characteristic sawtooth profile.

its return to the cryoplant. The need for a line 'D' for pressure relief in case of magnet quench is being evaluated.

A preliminary set of parameters for the proposed cooling scheme is shown in Table III for nominal operating conditions, *i.e.*, to handle steady-state heat loads, considering an arc cell length of 276 m [20], [21], and a cooling sector of 4.9 km. The longitudinal temperature gradient along a cell depends on the mass flow rate circulating in line 'A', while the radial temperature gradient (*i.e.*, from the cooling channel to the magnet coil itself) depends mostly on magnet/cold mass design, such as choice of solid materials, number of interfaces to cooling channel, and thermal contact resistance, along with the placement of the cooling channels (see Fig. 4). Since several designs for FCC-hh dipole magnets under study rely on pre-loading the coils via the cold mass outer shell, the placement of the cooling channels must be a compromise between proximity to the coil for effective heat extraction, and mechanical constraints.

TABLE III
MAIN PARAMETERS FOR THE PROPOSED CRYOGENIC COOLING SCHEME AT 4.5 K UNDER NOMINAL OPERATING CONDITIONS

| Parameter | Value |
|---|---|
| Line 'A' pressure [MPa] | 0.3 |
| Line 'A' minimum temperature [K] | 4.1 |
| Line 'A' maximum temperature [K] | 4.5 |
| Circulating mass flow rate [kg/s] | 0.5 |
| Saturation temp. at the re-coolers [K] | 4.0 |
| Maximum allowed temp. in coil [K] | 5.0 |
| Energy consumption [MW] | 139 |
| He inventory in cold mass [L/m] | 10 |
| Overall He inventory [tonnes] | 390 |
| Arc cell length [m] | 276 |
| Cryogenic cooling length [km] | 4.9 |
| Diameter of distribution line [mm] | <1000 |

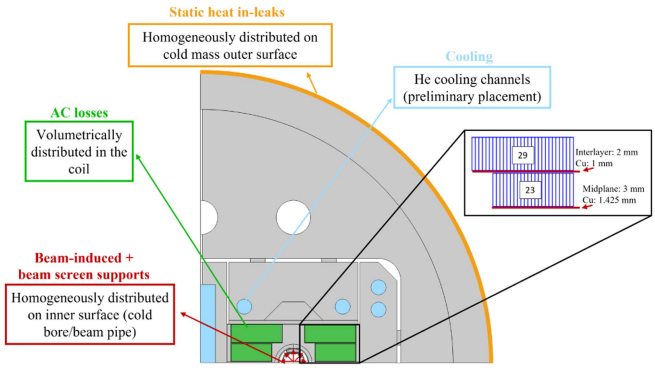


Fig. 4. Illustration of radial and longitudinal temperature gradients in the cooling circuit and within the magnet, exemplified on the cross-section of the BOND dipole magnet concept [22].

### F. Dealing With AC Losses

Solutions need to be investigated for handling the transient loads originated when powering the magnets, due to the unprecedented heat load generated by AC losses. As a reminder, the total heat load to the system during powering triples with respect to steady-state conditions with beam. At 4.5 K, the ≈3.5 t/m cold mass has a lumped specific heat capacity of roughly 2 J/(kg K): if an extra 0.5 K temperature excursion is allowed on the cold mass during powering (maximum coil temperature of 5.5 K), the cold mass itself can buffer 35% of the losses. To absorb the remaining 65% of energy dissipated, two options are currently under consideration: to increase the He inventory in the cold mass and use the available enthalpy of the helium to limit the temperature rise (as in the LHC), or to increase the circulating mass flow inside line 'A' and allow for extra evaporation in the re-coolers. Both options present operational challenges. If increasing the helium inventory, 30 L/m are needed to limit the temperature rise to 4.5 K, resulting in doubling the amount of helium stated in Table III and going back to a CDR-like He inventory. When opting for increasing the circulating mass flow and depleting the re-coolers, one risks increased helium losses and imbalance of the cryorefrigerator due to the increased evaporation rate at the re-cooling stations. Additionally, the re-coolers will need to increase in size to have enough autonomy for the powering phase, which can make their integration in the tunnel cumbersome.

## III. Radial Temperature Distribution: BOND Case Study

A preliminary study to estimate the magnitude of radial temperature gradients in a bladder-and-key cold mass structure was carried out using the BOND 14 T dipole cross-section [22], which was modified to incorporate thin copper strips in the interlayer and midplane areas to enhance radial heat transfer (1 mm and 1.4 mm, respectively, see Fig. 4). Two cooling configurations were considered:

- "Dry" (cooling channels): helium flow is confined to cooling pipes, placed as close as possible to the magnet coil in locations that do not disturb the transfer of forces by the interference keys; the inner free section is also transformed into a leak tight cooling duct. The cold mass and the coil itself are in a vacuum environment. The yoke and outer shell are cooled via the interference keys only;
- "Wet" (cross-flow): the helium stream flows freely through all openings in the cross-section, including added cooling channels. The coil is in direct contact with single-phase helium.

Both configurations are shown schematically in Fig. 5, where the blue zones represent helium flow. The fact that in the 'dry' configuration the coil sees insulation vacuum instead of a helium environment leads to concerns over dielectric breakdown of the magnet due to the Paschen effect [3]; if operation in vacuum becomes a showstopper, hybrid configurations where only the coil pack is surrounded by a small amount of helium can be envisaged in collaboration with magnet designers. Regarding heat loads, two cases were considered:

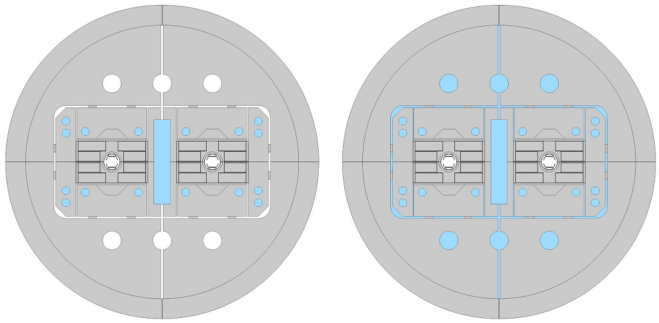


Fig. 5. Cooling configurations considered for radial temperature distribution study using the BOND dipole magnet concept [22]: (a) "dry" cooling channel configuration; (b) "wet" cross-flow configuration.

TABLE IV
Results of Temperature Profile Simulations Shown in Fig. 4, Considering $T_{He} = 4.5$ K

| Heat loads | Steady-state (1.4 W/m) | | Steady-state + ramping (4.5 W/m) | |
|---|---|---|---|---|
| Configuration | "Dry" | "Wet" | "Dry" | "Wet" |
| $T_{max}$, coil [K] | 4.72 | 4.72 | 5.14 | 5.13 |
| $T_{avg}$, coil [K] | 4.62 | 4.62 | 5.04 | 5.03 |
| $T_{max}$, cold mass [K] | 4.84 | 4.84 | 5.23 | 5.22 |
| $T_{avg}$, cold mass [K] | 4.61 | 4.51 | 4.65 | 4.54 |

- Steady-state: nominal operational static + dynamic heat loads from Table II, applied in the magnet cross-section as described in Fig. 4 (static heat inleaks, beam-induced, and beam-screen related components). This equals a total heat load of 1.37 W/m.
- Steady-state + ramping: to the above case, the AC losses generated inside the coil are added, distributed homogeneously in the coil volume (see Fig. 4). This equals a total heat load of 1.37 W/m + 3.13 W/m = 4.5 W/m.

The steady-state simulations were carried out in COMSOL Multiphysics for a helium temperature $T_{He} = 4.5$ K, worst-case condition expected in the last magnet in an arc cell, just before the re-cooler. This study is intended to give a preliminary estimate of the gradients to be expected considering literature values for thermal contact resistance between components and calculated heat transfer coefficients between the helium stream and the cooling channel walls. Details on fluid calculations, along with a detailed description of the thermal contact resistance model, are out of the scope of this work. As such, the results are best compared to each other, as they were computed using the same assumptions, rather than taken literally for their absolute value. The temperature distribution maps for the two cooling configurations and heat load cases are shown in Fig. 6, and Table IV summarises the maximum and average temperatures in the cross-section for each case. Convective heat flux boundary conditions with He temperature at 4.5 K were applied in the magenta lines of Fig. 6, and heat insulation conditions in the rest of the domain boundaries. The main observation is that there is hardly any difference between the 'dry' and 'wet' configurations in what concerns the coil temperature. The maximum and average cold mass temperatures are lower for the "wet" configuration, namely

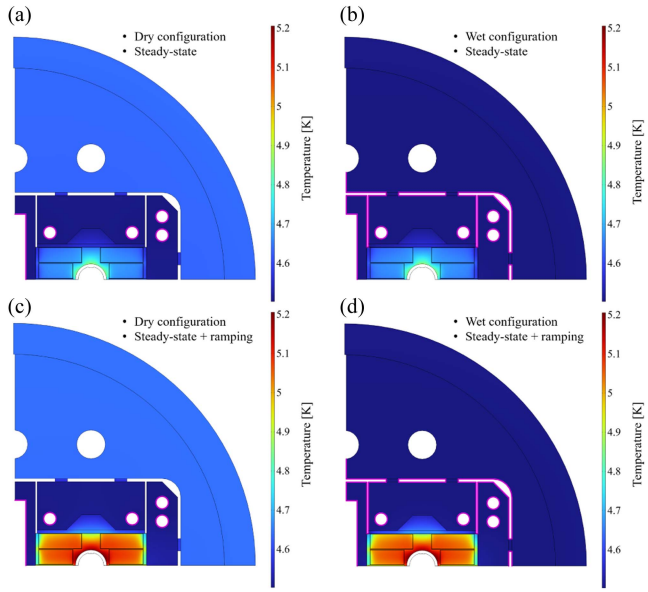


Fig. 6. Preliminary results of steady-state thermal simulations using COMSOL Multiphysics for the BOND cross-section, for two cooling configurations and two heat load scenarios; the highlighted zones in pink illustrate contact with the helium stream.

TABLE V
COMPARISON OF MAIN CRYOGENIC PARAMETERS CONSIDERING SCENARIO F14 FOR FCC-HH FOR 1.9 K AND 4.5 K

| FCC-hh Parameters | F14 at 1.9 K | F14 at 4.5 K 'Dry' |
|---|---|---|
| Magnet temperature [K] | 1.9 | 4.5 |
| Beam screen temperatures [K] | [40-60] | [40-60] |
| Number of sectors | 8 | 8 |
| Cryogenic capacity at 4.5 Keq [kW] | 1040 | 698 |
| Number of cryoplants | 16 | 16 |
| Electrical consumption [MW] | 206 | 139 |
| Helium inventory [tonnes] | 820 | 390 |

the yoke, which can be important depending on the placement of splices, busbars, etc., but is otherwise inconsequential to the coil and its available temperature margin. The maximum coil temperature in the "dry" configuration for the nominal (steady-state) heat load is 4.72 K, i.e., a 0.2 K gradient with respect to the helium stream; however, assuming otherwise the same conditions, the coil's maximum temperature rises to above 5.1 K when the heat loads due to powering are added. This value is slightly above the design parameter of 5 K outlined by the HFM programme and its effect on the magnet's available temperature margin needs to be assessed.

The advantages of having a fully wetted magnet cross-section on the maximum coil temperature are marginal: while the 'wet' configuration has enough He content to act as an enthalpy reservoir and buffer the ramping losses, it has no visible advantage in locally extracting the heat from the coil pack. The peak temperature in the coil depends heavily on the thermal contact resistance between solid parts, on the thermal conductivity of the constituents of the coil pack, and on the overall composition and thickness of the coil impregnation and ground insulation, and much less on the local heat transfer coefficient of the helium stream or on the placement of the cooling channels. As the design of the cryogenic cooling scheme and magnet evolves, the radial temperature profiles can be recalculated and help drive an effective compromise between the cold mass' mechanical and thermal design.

## IV. CONCLUSION

An alternative cooling layout for the FCC-hh machine that uses forced flow of single-phase helium at around 4.5 K through cooling channels embedded in the cold mass has been presented. It provides a suitable thermal environment for the 14 T $Nb_3Sn$ magnets, limiting the longitudinal temperature gradients to 0.4 K over an arc cell and the radial gradients to 0.5 K, which can be optimized as the magnet as well as the cryogenic designs mature in close collaboration. Table V compares the baseline cooling at 1.9 K with the proposed 'dry' layout at 4.5 K in terms of installed cryogenic capacity, electrical consumption, and helium inventory.

The 'dry' layout has the potential to reduce the installed cryogenic capacity by 30%, which reduces capital costs, and the electrical consumption also by 30%, reducing operational costs over the collider's lifetime. The overall helium inventory may be reduced by 50%, which simplifies logistics, tunnel access, and personnel safety. Furthermore, most of the helium is confined to discrete points in the accelerator tunnel, in the re-cooling stations, and not in direct contact with the magnet's cold mass, potentially simplifying the helium management in case of a quench. The penalty in recovery time after a quench, and details on how to isolate the quenched cell and prevent it from disturbing the rest of the sector are part of the ongoing study.

Raising the maximum allowed temperature in the coil from the currently assumed 5 K to 5.5 K would allow for the saturated bath temperature in the re-coolers to be raised to ≈4.2 K (saturation pressure 0.1 MPa), thus eliminating the need for a cold compressor on the pumping line, and allowing the entire system to be operated at ambient or slight overpressure. Suppressing the need for a sub-atmospheric line 'B' can simplify manufacturing requirements and quality assurance of the cryogenic distribution line. If the FCC-hh dipoles are designed with sufficient temperature margin to allow a maximum temperature of 5.5 K, the gains in the cryogenic infrastructure are tangible, with a direct impact not only on capital and running costs but also on the accelerator cryogenic system's availability.

Next steps involve a detailed study of the transient modes of the system such as cooldown and quench recovery, and consolidation of the method to buffer the transient heat loads due to magnet ramping in the machine's nominal cycle.

## REFERENCES

[1] M. Benedikt et al., "Future circular collider feasibility study report volume 2," CERN, Geneva, Switzerland, Tech. Rep., 2025. [Online]. Available: https://cds.cern.ch/record/2928793
[2] F. Zimmermann, "FCC-hh studies for the next European strategy: Energy, luminosity, operation scenarios," Indico, 2024. [Online]. Available: https://indico.cern.ch/event/1439072/contributions/6106995/
[3] B. Auchmann et al., "High field magnet programme–European strategy input," 2025, *arXiv:2504.16885*.

[4] E. Todesco, "Status and perspectives of high field magnets for particle accelerators," *IEEE Trans. Appl. Supercond.*, vol. 35, no. 5, Aug. 2025, Art. no. 4003914.

[5] A. Abada et al., "FCC-hh: The hadron collider," *Eur. Phys. J. Special Topics*, vol. 228, no. 4, pp. 755–1107, Jul. 2019, doi: 10.1140/epjst/e2019-900087-0.

[6] O. S. Brüning et al., "CERN yellow reports: Monographs," CERN, Geneva, Switzerland, LHC Des. Rep., 2004. [Online]. Available: https://cds.cern.ch/record/782076

[7] S. Claudet et al., "1.8 k refrigeration units for the LHC: Performance assessment of pre-series units," LHC-Project-Report-797, 2005. [Online]. Available: https://cds.cern.ch/record/795007

[8] H. Gruehagen and U. Wagner, "Measured performance of four new 18 kW, 4.5 k helium refrigerators for the LHC cryogenic system," no. LHC-Project-Report-796, 2005. [Online]. Available: https://cds.cern.ch/record/795005

[9] S. I. Bermudez, "Persistent current magnetization effects in the 16 T main dipoles for the future circular collider," Tech. Rep. Internal Note EDMS 2036614, CERN, Geneva, Switzerland, 2018. [Online]. Available: https://edms.cern.ch/document/2036614/2

[10] M. Murakami and K. Harada, "Experimental study of thermo-fluid dynamic effect in He II cavitating flow," *Cryogenics*, vol. 52, no. 11, pp. 620–628, 2012. [Online]. Available: https://www.sciencedirect.com/science/article/pii/S0011227512001646

[11] R. V. Smith, "Review of heat transfer to helium I," *Cryogenics*, vol. 9, no. 1, pp. 11–19, 1969. [Online]. Available: https://www.sciencedirect.com/science/article/pii/0011227569902513

[12] A. Onufrena et al., "Remote cooling systems with mesh-based heat exchangers for cryogenic applications," *IOP Conf. Ser., Mater. Sci. Eng.*, vol. 1240, no. 1, Art. no. 012049, May 2022, doi: 10.1088/1757-899X/1240/1/012049.

[13] J. Wu et al., "Investigation of heat transfer and pressure drop of $CO_2$ two-phase flow in a horizontal minichannel," *Int. J. Heat Mass Transfer*, vol. 54, no. 9/10, pp. 2154–2162, 2011. [Online]. Available: https://www.sciencedirect.com/science/article/pii/S0017931010006897

[14] D. Delikaris and L. Tavian, "The LHC cryogenic system and operational experience from the first three years run," *J. Cryogenics Supercond. Soc. Jpn.*, vol. 49, no. 12, pp. 590–600, 2014.

[15] S. W. Van Sciver, *Helium Cryogenics* (International Cryogenics Monograph Series). New York, NY, USA: Springer, 2012. [Online]. Available: https://cds.cern.ch/record/1444601

[16] J. D. Jackson, R. G. Barton, and R. Donaldson, "Conceptual design of the superconducting super collider," Lawrence Berkeley Lab., SSC Central Des. Group, Berkeley, CA, USA, Tech. Rep. 03, 1986. [Online]. Available: https://www.osti.gov/biblio/10123370

[17] M. A. Iarocci et al., "RHIC cryogenics," *Nucl. Instrum. Methods Phys. Res. Sec. A*, vol. 499, no. 2, pp. 264–279, 2003. [Online]. Available: https://www.sciencedirect.com/science/article/pii/S0168900202019393

[18] H. R. Barton et al., "The refrigeration system for the superconducting proton ring of the electron proton collider HERA," in *Advances in Cyrogenic Engineering*. Boston, MA, USA: Springer, 1986, vol. 31, pp. 635–645, doi: 10.1007/978-1-4613-2213-9_72.

[19] C. H. Rode, "Tevatron cryogenic system," *Conf. Proc. C*, vol. 830811, pp. 529–535, 1983.

[20] G. Perez-Segurana, E. Todesco, and M. Giovannozzi, "Study of the corrector systems for the new lattice of the CERN hadron-hadron future circular collider," in *Proc. 15th Int. Part. Accel. Conf.*, Geneva, Switzerland, May 2024, vol. 15, pp. 79–82. [Online]. Available: https://indico.jacow.org/event/63/contributions/3396

[21] G. Perez-Segurana et al., "A new baseline layout for the FCC-hh ring," in *Proc. 15th Int. Part. Accel. Conf.*, Geneva, Switzerland, May 2024, vol. 15, pp. 75–78. [Online]. Available: https://indico.jacow.org/event/63/contributions/3331

[22] J. C. Perez et al., "Conceptual design of BOND: A 14 T dipole for FCC-hh," *IEEE Trans. Appl. Supercond.*, vol. 35, no. 5, Aug. 2025, Art. no. 4002506.